NDT&E International 141 (2024) 102993

Contents lists available at ScienceDirect

NDT and E International

journal homepage: www.elsevier.com/locate/ndteint

Frequency dependent amplitude response of different couplant materials for mounting piezoelectric sensors

Ronghua Xu [a,*], Raúl Enrique Beltrán-Gutiérrez [a], Max Käding [b], Alexander Lange [c], Steffen Marx [a], Jörn Ostermann [c]

[a] Institute of concrete structures, Technische Universität Dresden, August-Bebel-Straße 30, Dresden 01219, Germany
[b] MKP GmbH, Zum Hospitalgraben 2, Weimar 99425, Germany
[c] Institute for information processing, Leibniz Universität Hannover, Appelstraße 9A, Hannover 30167, Germany

ARTICLE INFO

Keywords:
Non-destructive testing (NDT)
Couplant material
Laser Doppler vibrometer
Acoustic emission (AE)
Signal transmission

ABSTRACT

Non-destructive testing techniques, such as ultrasonic testing and acoustic emission analysis, commonly employ piezoelectric sensors for monitoring and detecting defects in structures. The quality of data acquired using these sensors is highly dependent on the coupling layer between the transducer and the structure's surface. In this context, this study compares the signal response of four different couplant materials, namely acrylic adhesive pads, honey, vaseline, and hot glue, applied to a steel surface. For this purpose, experiments were conducted using a laser Doppler vibrometer and acoustic emission analysis to investigate the signal transmission of the couplant materials and their impact on the signal response of a coupled piezoelectric sensor VS30-V. The repeatability of the experiments was statistically analyzed. The findings indicate that acoustic emission measurements with acrylic adhesive pads exhibited the lowest relative standard deviation of 11.4%, followed by honey (13.2%), hot glue (21.9%), and vaseline (32.1%). The investigated couplant materials exhibited different effects on the signal response of the piezoelectric sensor. Specifically, acrylic adhesive pads and hot glue demonstrated more reliable signal transmission in the frequency range of 50 kHz to 65 kHz. In contrast, honey and vaseline had better performance within the frequency range of 65 kHz and 80 kHz. Considering the frequency-dependent characteristics of signal transmission and the ease of application, acrylic adhesive pads and honey are considered the preferred couplant materials for the frequency ranges of 50 kHz to 65 kHz and 65 kHz to 80 kHz, respectively.

1. Introduction

For several decades, non-destructive testing (NDT) methods have been employed in civil engineering to inspect and assess various structures and materials [1–4]. In NDT techniques such as ultrasonic testing and acoustic emission (AE) testing, the use of piezoelectric sensors that exploit the piezoelectric effect of lead zirconate titanate (PZT), is prevalent [5,6]. Piezoelectric sensors, which are constructed with piezoelectric materials such as ceramics or polymers, possess the inherent ability to produce electrical charges in response to mechanical stress or deformation. The resulting electrical charge is amplified and processed by the sensor's electronic circuitry, enabling the generation of a signal that can be displayed and analyzed by measuring equipment. It is known that the acoustic impedance of air is significantly lower than that of piezoelectric materials [7], leading to a substantial proportion of signals being reflected back and consequently decreasing the measurement sensitivity. In order to enhance signal transmission, it is common practice to place a couplant layer between the sensor and the object being tested [8–10]. This ensures that the sensor is in direct contact with the object and eliminates any air gaps thereby improving the transmission of mechanical energy and reducing energy loss due to impedance mismatch. Although the use of couplant materials effectively enhances signal transmission between the contact surface and the sensor, it also introduces some degree of variability, as different couplant materials may exhibit different transmission properties [11–13]. The properties of the used couplant materials can have a substantial impact on the quality and repeatability of the generated sensor output [14]. In [15], the authors performed impact-echo measurements on concrete probes to analyze the signal response of a PCB piezoelectric sensor coupled with various couplant materials in the low-frequency range of 0 to 5 kHz. Similarly, in [16], the authors investigated the effect of different couplant materials, such as glycerin and propylene glycol, on the sensitivity of a broadband piezoelectric sensor (20 kHz–1 MHz) to both longitudinal and shear waves on an aluminum test block.

* Corresponding author.
E-mail address: ronghua.xu@tu-dresden.de (R. Xu).

https://doi.org/10.1016/j.ndteint.2023.102993
Received 3 July 2023; Received in revised form 28 October 2023; Accepted 5 November 2023
Available online 10 November 2023

(a) (b) (c) (d)

Fig. 1. The chosen couplant materials for experiments: (a) acrylic adhesive pads manufactured by Meiz Tech GmbH, (b) hot glue manufactured by Bosch, (c) vaseline manufactured by Bombastus-Werke AG, and (d) honey manufactured by Dr. Krieger's.

In our previous research [17], we employed VS30-V type piezoelectric sensors, manufactured by Vallen, to detect wire break-like signals in post-tensioned tendons through AE analysis. These sensors were applied to various structure elements, including concrete beams and steel plates. It was observed that the coupling of the sensors played a significant role in ensuring data quality. In this paper, we comprehensively investigate the frequency-dependent signal response of various couplant materials and their effects on the performance of aforementioned type of piezoelectric sensor using Fourier Transform components. This study comprises two sets of experiments: In Section 2.2.1, optical measurements using a laser Doppler vibrometer are presented. The aim of these measurements is to determine the frequency-dependent amplitude response of couplant materials when stimulated by ultrasonic signals. In Section 2.2.2, AE measurements that investigate the signal transmission of a piezoelectric sensor coupled with the tested materials are described. The obtained results are expounded in Section 3, along with an exhaustive explanation of the post-processing procedure for the measured signals presented in Section 3.1. Furthermore, the repeatability of the experiments conducted with different couplant materials is demonstrated in Section 3.2, and the transfer functions of both isolated couplant materials and the coupled sensor are compared in Section 3.3. These couplant materials are evaluated in terms of signal transmission capabilities and ease of application.

2. Experiments

2.1. Materials

This study aims to investigate the signal transmission of various couplant materials, both in isolation and when coupled with a piezoelectric sensor. To this end, four substances were carefully selected and representative products from commonly available brands were chosen for each substance (Fig. 1):

The authors acknowledge that the thickness of the couplant materials can affect the sensor response. However, to replicate realistic in-situ conditions, the couplant thickness was not deliberately controlled in this study. For the experiments involving vaseline and honey, a thin couplant layer was applied using a spatula. The acrylic adhesive pads were manufactured with a consistent thickness of 0.5 mm and remained unchanged throughout the experiments. Hot glue was exclusively used in the second part of the study, as it was only feasible to achieve a uniform thickness of this couplant material when it was combined with a sensor under pressure.

2.2. Methods

2.2.1. Laser Doppler vibrometer

The main objective of the experiments presented here is to investigate the frequency-dependent amplitude response of diverse couplant materials when stimulated by ultrasonic signals. To achieve this, measurements were conducted on a steel block measuring 24 cm × 10 cm × 2 cm, as shown in Fig. 2(a). Fig. 2(b) depicts the experiment setup, wherein an ultrasonic transducer model Olympus V101-RB, featuring a broad frequency range of 50 kHz to 1 MHz, was bonded to the center of the steel block with acrylic adhesive pads. On the opposite side, a digital single-point laser Doppler vibrometer Nova-Speed-DF, equipped with an invisible short wavelength infrared (SWIR) laser (1550 nm), was aligned with its optical beam normal to the steel block along the central axis.

The V101-RB transducer, manufactured by Olympus, was stimulated using a discrete frequency sweep generated by a RITEC SNAP RAM 5000 ultrasonic wave generator. The sweep consisted of sinusoidal burst signals with a pre-defined width of 0.4 ms, covering frequencies ranging from 50 kHz to 1 MHz in increments of 5 kHz, as depicted in Fig. 3. A laser Doppler vibrometer was employed to detect the out-of-plane velocity component of the longitudinal wave propagated through the steel block. The analog output signal was acquired at a sampling rate of 80 MHz using a PicoScope 4424 A oscilloscope, with the measurement being triggered synchronously with the ultrasonic wave generator. Upon transmission of the input signal, the oscilloscope commenced recording. Each signal within the frequency sweep was measured for a duration of 0.2 ms. To assess the repeatability of the experiments, five repetitions were performed on the steel block for each couplant material. Additionally, a reference measurement was performed in the absence of any couplant materials on the measuring side. Employing the same input frequency sweep and experimental setup, the out-of-plane velocity on the bare steel surface was quantified using the laser Doppler vibrometer.

Given that our system operates under small deformations and for a brief duration, it can be considered a linear time-invariant (LTI) system. By applying the linear filter theory from systems theory, the response of a system can be determined through an analysis of the transfer functions of its components within the measurement [18–20]. Based on this approach, the frequency spectrum of the output signal $Rec_{laser}(f)$ obtained from the measurement chain depicted in Fig. 2(b) can be described by the transfer functions of the coupled ultrasonic transducer, steel block, and couplant material, as well as the input burst signals denoted in Eq. (1) as $TF_{ut}(f)$, $TF_s(f)$, $TF_c(f)$ and $S(f)$, respectively:

$$Rec_{laser}(f) = S(f) \cdot TF_{ut}(f) \cdot TF_s(f) \cdot TF_c(f) \tag{1}$$

For the reference measurement on the bare steel surface, the subsequent equation can be derived:

$$Rec_{ref}(f) = S(f) \cdot TF_{ut}(f) \cdot TF_s(f) \tag{2}$$

where $Rec_{ref}(f)$ represents the frequency spectrum of the recorded output signal from the reference measurement. By substituting Eq. (2) into Eq. (1), the influence of measuring elements such as the steel block and the ultrasonic transducer can be eliminated. Following this elimination process, properties of the steel block such as the material composition and thickness, will not affect the comparative analysis of couplant materials, which will be discussed in subsequent sections. However, it is still necessary to control it within a certain range to ensure a high quality of received signals. Further discussion on transfer block thickness can be found in [21]. The transfer function of the couplant material $TF_c(f)$ can be expressed as follows:

$$TF_c(f) = \frac{Rec_{laser}(f)}{Rec_{ref}(f)} \tag{3}$$

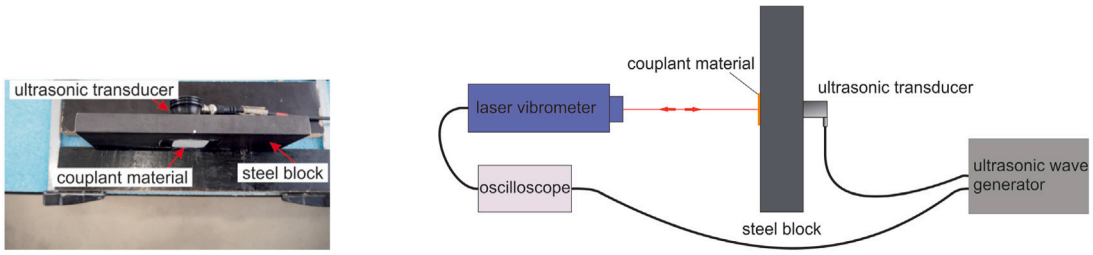

Fig. 2. (a) Experimental setup for measuring the frequency-dependent amplitude response of couplant materials when stimulated by ultrasonic signals; (b) Illustrated diagram of the measuring chain.

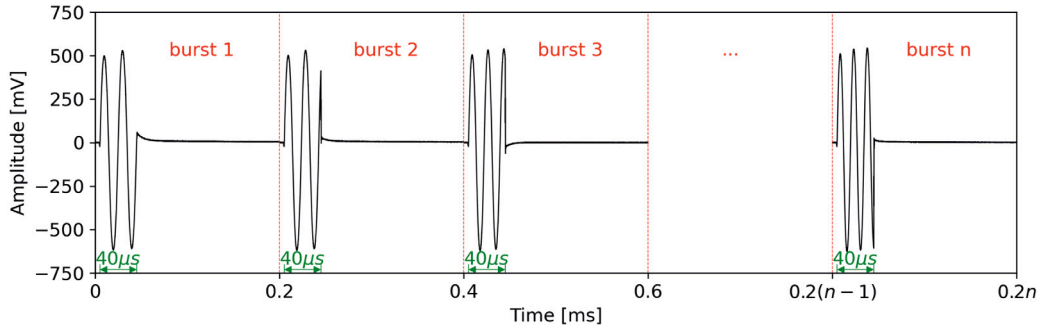

Fig. 3. Discrete frequency sweep of sinusoidal burst signals produced by the RITEC SNAP RAM 5000 ultrasonic wave generator spanning a frequency range from 50 kHz to 1 MHz with a step width of 5 kHz.

The out-of-plane velocity $Rec(t)$ measured by the laser Doppler vibrometer was digitized and stored as a discrete-time sequence. To obtain the corresponding frequency spectrum $Rec(f)$, Discrete Fourier Transform (DFT) was applied to $Rec(t)$:

$$Rec(f) = \mathcal{F}\{Rec(t)\} = \sum_{n=0}^{N_{laser}-1} Rec(n \cdot \Delta t_{laser}) \cdot e^{-2\pi f i n \Delta t_{laser}} \quad \text{with } f = \frac{m}{N_{laser} \cdot \Delta t_{laser}} \quad (m = 0, 1, 2, \ldots, N_{laser} - 1) \tag{4}$$

Here, N_{laser} represents the number of samples and Δt_{laser} denotes the sampling interval of the experiments conducted using the laser Doppler vibrometer. The obtained complex value of $Rec(f)$, derived from Eq. (4), is simplified by considering only its amplitude for the calculation of the transfer function. Consequently Eq. (3) can be formulated as follows:

$$TF_c(f) = \frac{|\sum_{n=0}^{N_{laser}-1} Rec_{laser}(n \cdot \Delta t_{laser}) \cdot e^{-2\pi f i n \Delta t_{laser}}|}{|\sum_{n=0}^{N_{laser}-1} Rec_{ref}(n \cdot \Delta t_{laser}) \cdot e^{-2\pi f i n \Delta t_{laser}}|} \quad \text{with } f = \frac{m}{N_{laser} \cdot \Delta t_{laser}} \quad (m = 0, 1, 2, \ldots, N_{laser} - 1) \tag{5}$$

2.2.2. Acoustic emission measurements

In practical applications, couplant materials are typically used in conjunction with sensors. The second part of the experiments aimed to investigate the influence of various couplant materials on the signal transmission of an AE sensor. For this purpose, a piezoelectric sensor VS30-V, manufactured by Vallen Systeme GmbH, was utilized as the receiver. According to the manufacturer's datasheet, this sensor has a primary measuring frequency range of 25 to 80 kHz and weighs 69 g. It was affixed on the center of the steel block with a magnetic holder, which provided a constant pressure force of approximately 50 N, and connected to an AE system AMSY6 without preamplification. The experimental setup is shown in Fig. 4. The experiments were conducted using the same source signals as described in Section 2.2.1. A bandpass filter with a range of 25 to 850 kHz was applied, and the out-of-plane displacement was measured by the AE system at a sampling rate of 5 MHz. To access the repeatability, the experiments were repeated five times for each couplant material. Unlike the input ultrasonic signals spanning a frequency range from 50 kHz to 1 MHz, the chosen sensor had a significantly restricted measuring range. This low-frequency piezoelectric sensor was selected for the present study due to its widespread use in monitoring and detecting defects in large structures such as bridges. The primary objective of this investigation is to identify the frequency response of this specific sensor when coupled with diverse materials and to provide guidance for the optimal selection of appropriate couplant materials for in-situ applications.

Analogous to Eq. (1), the system response of the AE measurement in the frequency domain can be expressed as follows:

$$Rec_{ae}(f) = S(f) \cdot TF_{ut}(f) \cdot TF_s(f) \cdot TF_{ae}(f) \tag{6}$$

Here, $Rec_{ae}(f)$, $S(f)$, $TF_{ut}(f)$, $TF_s(f)$, $TF_{ae}(f)$ represent the recorded output signal of the AE measurement, the input burst signal, the transfer functions of the coupled ultrasonic transducer, the steel block and the coupled AE sensor, respectively. By substituting Eq. (2) into Eq. (6), the transfer function of the coupled sensor can be derived as follows:

$$TF_{ae}(f) = \frac{Rec_{ae}(f)}{Rec_{ref}(f)} \tag{7}$$

To obtain the frequency response $Rec_{ae}(f)$ of the AE measurement, DFT as described in Eq. (4) should be applied. Notably, ensuring a meaningful comparison between $Rec_{ae}(f)$ and $Rec_{ref}(f)$ requires the number of samples N and the sampling interval Δt to be consistent for both the reference and AE measurements. This can be fulfilled through data post-processing as detailed in Section 3.1. Consistent with the simplification employed for the transfer function of couplant materials, as described in Eq. (5), the transfer function of the coupled sensor is also simplified by considering only the magnitude of the frequency response. Hence, Eq. (7) can be rewritten as follows:

$$TF_{ae}(f) = \frac{|\sum_{n=0}^{N-1} Rec_{ae}(n \cdot \Delta t) \cdot e^{-2\pi f i n \Delta t}|}{|\sum_{n=0}^{N-1} Rec_{ref}(n \cdot \Delta t) \cdot e^{-2\pi f i n \Delta t}|} \quad \text{with } f = \frac{m}{N \cdot \Delta t} \quad (m = 0, 1, 2, \ldots, N - 1) \tag{8}$$

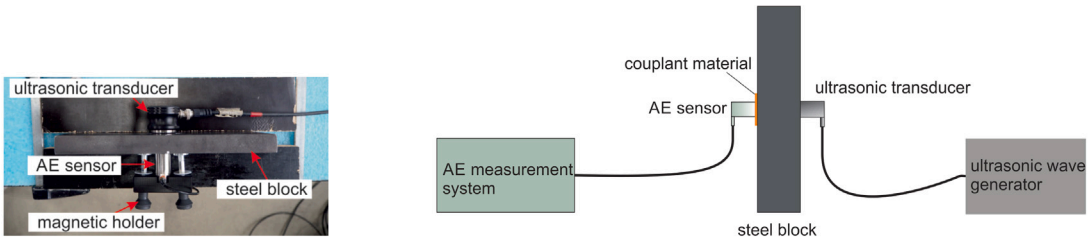

Fig. 4. (a) Experimental setup for measuring the frequency response of the piezoelectric sensor when coupled with different materials; (b) Illustrated diagram of the measuring chain.

Here, N denotes the number of samples obtained from both the laser Doppler vibrometer and the post-processed AE measurements, while Δt represents the consistent sampling interval for both sets of measurements. It is important to emphasize that the reference and the AE measurements were performed using distinct systems. Therefore, the transfer function of the coupled sensor presented in Eq. (8) should only be interpreted in a comparative context among the couplant materials investigated. Previous studies have also reported the utilization of a laser Doppler vibrometer or laser interferometer as a reference for the calibration of piezoelectric sensors [21–23].

In the current experiments, achieving time synchronization between the AE measurements and the ultrasonic generator was not feasible, unlike those conducted with the laser Doppler vibrometer. To circumvent this issue, a threshold of 60 dB was set for the AE measurements, based on the background noise level, to capture only the pertinent burst signals. Upon the initiation of the AE measurements, the source burst signals were transmitted from the ultrasonic generator. The first input signal produced by the ultrasonic generator corresponds to the first output signal received by the AE system. Consequently, in keeping with the principle that the time intervals between transmitted ultrasonic waves should be consistent with those of received signals, the pertinent output signals are selected for the purpose of evaluation.

3. Results and discussion

3.1. Signal post-processing

This section describes the signal post-processing methodology employed in the experiments, using vaseline as an example of a representative couplant material. The post-processing steps were consistently applied to all obtained signals. The raw data pertaining to all mentioned laser Doppler vibrometer and AE measurements can be found in dataset [24]. The input signals had a fixed burst width of 0.04 ms and a signal delay of 0.005 ms. They were emitted from the ultrasonic generator at pre-defined frequencies ranging from 50 kHz to 1 MHz with a step width of 5 kHz. For each input burst signal, corresponding output signals were recorded using the laser Doppler vibrometer and the AE system. These signals were subsequently digitized and stored as discrete electrical voltages in the time domain. The signals at varying frequencies may exhibit non-integer periods within the fixed burst width, resulting in a phenomenon known as frequency leakage. To mitigate the leak effect in the amplitude spectrum, a Hann window was applied to the signals. Fig. 5 illustrates the post-processing procedure using an example of a 60 kHz input signal, along with the corresponding output signals obtained by the two systems mentioned above.

Discrimination between signal and noise components within output signals presents a significant challenge. To ensure consistency and minimize manual intervention during signal post-processing, a Hann window was implemented over the entire measuring period, ranging from 0 to 0.2 ms, for output signals obtained from both the laser Doppler vibrometer and the AE system. Notably, the laser Doppler vibrometer output signals had a time delay of approximately 0.05 ms prior to initiation. This lag is attributed to the processing time required by the laser Doppler vibrometer to analyze received signals. To assess the system's response at the input frequency, the corresponding magnitude of the output signal was extracted from the amplitude spectrum and utilized for the subsequent transfer function analysis in Section 3.3. As shown in Fig. 5, the laser Doppler vibrometer output exhibited an amplitude of 0.62 mV at the designated input frequency of 60 kHz. Compared to the amplitude of the input signal, which recorded 28.75 mV, a substantial attenuation of the transmitted signal can be observed.

In the AE measurements, the transient AE signal was recorded until the set threshold was no longer exceeded. However, the complete AE signal included not only the incident wave but also numerous reverberations resulting from sensor vibration during signal recording. Due to the challenge of distinguishing between the incident wave and reverberations, it is assumed that the AE signal, spanning the same duration as the input signal (0–0.2 ms), represents the transmitted incident wave. Based on this assumption, the transfer function of the AE sensor coupled with the different materials can be defined using Eq. (8). As mentioned in Section 2.2.2, the sampling frequency of the AE system was 5 MHz, while that of the laser Doppler vibrometer was 80 MHz. Since an equal sampling frequency is required for the calculation of the transfer function in Eq. (8), the AE signal was resampled at the same sampling frequency as the laser Doppler vibrometer. The resampling procedure was executed using the Inverse Fast Fourier Transformation (IFFT). By applying the same Hann window used for laser Doppler vibrometer experiments, the post-processed signal and its amplitude spectrum are shown in Fig. 5. In contrast to measurements conducted solely on couplant materials using the laser Doppler vibrometer, the AE measurement performed on a coupled sensor produced significantly larger output signals. At the frequency of 60 kHz for the example input signal, an amplitude of 59.14 mV was observed for the AE output, which was approximately twice the amplitude of the input signal. This observation aligns with the fundamental working principle of AE sensors, which are designed to detect and amplify very small signals.

3.2. Repeatability of the measurements

Multiple test configurations with different couplant materials were used to perform the measurements, as detailed in Section 2.2. Based on the five repetitions for each test configuration, the relative standard deviation (RSD) of the measured signals representing the variability of experiments was computed. The RSD is employed as a statistical indicator of repeatability and is calculated by determining the standard deviation relative to the mean. To investigate the frequency-dependent repeatability, the mean RSD for a specific frequency range was computed by averaging the RSD values obtained at each individual frequency point within the given range. Table 1 displays the computed mean RSD values for all test configurations across various frequency ranges. Among the tested materials in the laser Doppler vibrometer measurements, the experiments on vaseline demonstrated the highest

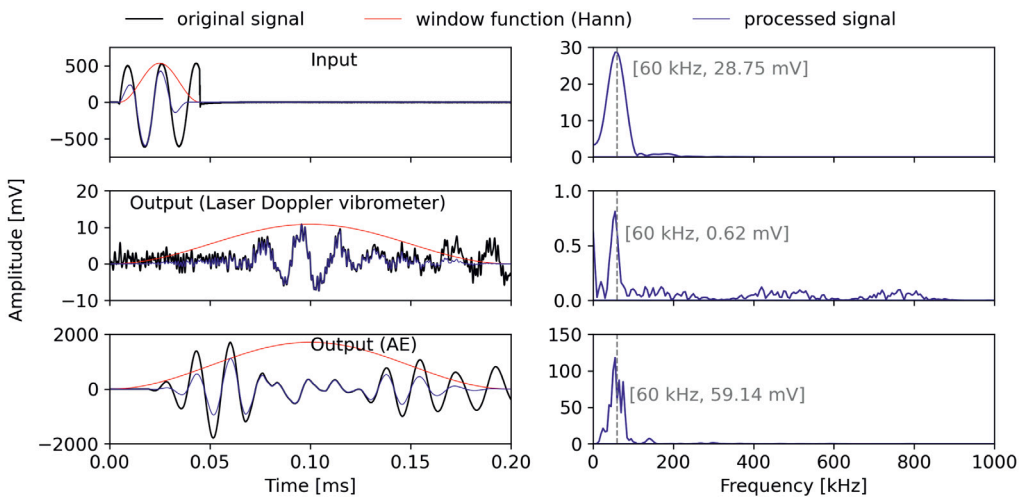

Fig. 5. An illustration of signal post-processing applied to input and output signals, demonstrated through measurements conducted on vaseline stimulated by a 60 kHz input signal.

Table 1
Mean relative standard deviation of output signals measured by laser Doppler vibrometer and AE system.

Measurement	Measured object	Mean relative standard deviation of output signals [%]						
		50–100 kHz	100–250 kHz	250–400 kHz	400–550 kHz	550–700 kHz	700–850 kHz	850–1000 kHz
Laser Doppler vibrometer	Acrylic adhesive pads	9.7	18.7	20.7	21.3	11.4	13.5	39.8
	Honey	21.3	28.3	32.9	36.9	40.6	34.7	77.6
	Vaseline	30.6	35.0	54.5	50.6	49.2	47.8	71.6
AE system	VS30-V + Acrylic adhesive pads	11.4	20.1	10.4	16.3	13.4	29.4	–
	VS30-V + Hot glue	21.9	27.1	22.5	33.9	45.8	44.5	–
	VS30-V + Honey	13.2	29.6	12.8	15.7	14.1	16.1	–
	VS30-V + Vaseline	32.1	30.0	30.0	30.1	27.9	29.4	–

RSD, exceeding 30% over a broad frequency range from 50 kHz to 850 kHz. This can be attributed to the lower viscosity of vaseline, leading to uneven coupling during the experimental procedures. In contrast, the output signals obtained from the acrylic adhesive pads exhibited the lowest RSD of 9.7%, indicating superior repeatability. This can be explained by the fixed thickness and stable form of the adhesive pads. Upon comparing the two sets of experiments, it is noteworthy that in the AE measurements, the output signals for honey and vaseline displayed relatively lower RSD values compared to those observed in the laser Doppler vibrometer experiments. Notably, the RSD for honey was reduced from 21.3% to 13.2% within the low-frequency range of 50 kHz to 100 kHz. This reduction can be attributed to the consistent pressure applied to the sensor using a magnetic holder in the AE measurements. However, the RSD for experiments on hot glue did not demonstrate comparable performance, despite the application of the same magnetic holder. A plausible explanation lies in the raid hardening of hot glue, which limited the available time for precise positioning or adjustment, consequently introducing uncontrollable variations between experiments.

In addition to the mean RSD values in Table 1, the comprehensive distribution analysis of the output signals over the input frequencies is presented in Fig. 6 for the laser Doppler vibrometer measurements and in Fig. 7 for the AE measurements. As shown in Fig. 6, the output signals measured by the laser Doppler vibrometer measurements with different couplant materials revealed minor variations compared to the reference experiment. Notably, a prominent peak around 150 kHz is observed in all cases, suggesting that this frequency corresponds to the eigenfrequency of the test setup. Fig. 7 shows the amplitude spectra of the output signals for the AE measurements with different couplant materials. Specifically, within the primary measuring range of the AE sensor VS30-V (25 kHz–80 kHz), two peaks at 60 kHz and 75 kHz are observed for the acrylic adhesive pads and hot glue with amplitudes of approximately 150 mV and 20 mV, respectively. Similarly, honey and vaseline also exhibited two peaks in their amplitude spectra. The first peak is observed at 55 kHz, displaying comparable output values to those of the acrylic adhesive pads and hot glue. However, the second peak at 75 kHz demonstrated significantly higher amplitudes, ranging from approximately 150 mV to 200 mV, surpassing the response observed for the acrylic adhesive pads and hot glue. The attenuated response of the acrylic adhesive pads and hot glue at 75 kHz can be attributed to the thick layer of these materials, which influenced the transmission and detection of higher frequencies. For frequencies beyond the main measuring range of the AE sensor, the output signals recorded using the acrylic adhesive pads and hot glue exhibited minimal amplitudes, while honey and vaseline maintained relatively higher values, particularly below 200 kHz.

3.3. Transfer function

Using Eq. (5), the transfer function of each couplant material was determined through the division of its mean output by the output of the reference measurement (Fig. 6). Fig. 8 shows the obtained transfer functions. In general, the transfer functions were mostly close to one across the entire frequency range from 50 kHz to 1 MHz, indicating that the input signals were not attenuated significantly by the couplant materials. Fig. 9 provides a more detailed analysis of the attenuation patterns of the received signals with different couplants. Here, attenuation is represented by negative values while amplification is denoted by positive values. Notably, the attenuation was less than −5 dB over the entire frequency range. However, some deviations were observed at certain frequencies. In particular, at around 220 kHz and above 850 kHz, all couplant materials exhibited a sudden and significant increase in signal transmission, with amplification values ranging from 10 to 20 dB. This phenomenon was probably caused by the extremely

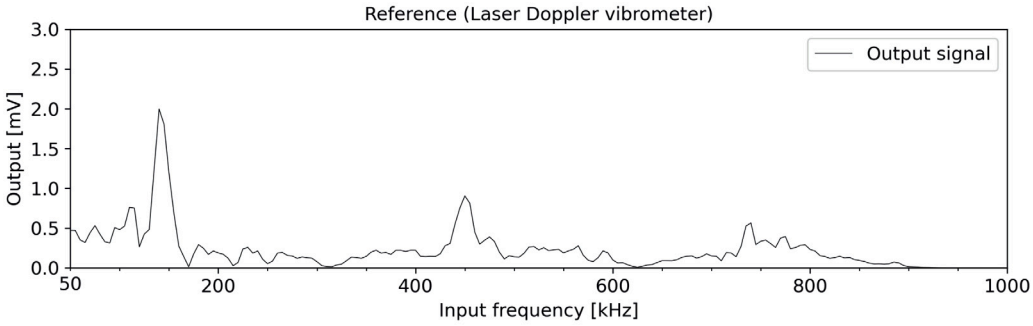

(a)

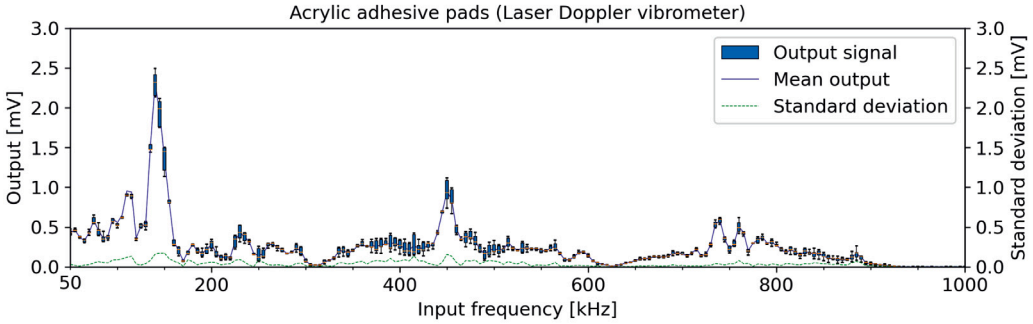

(b)

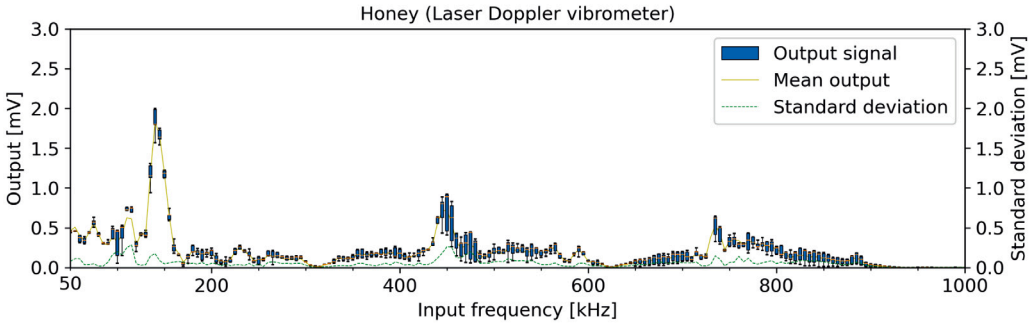

(c)

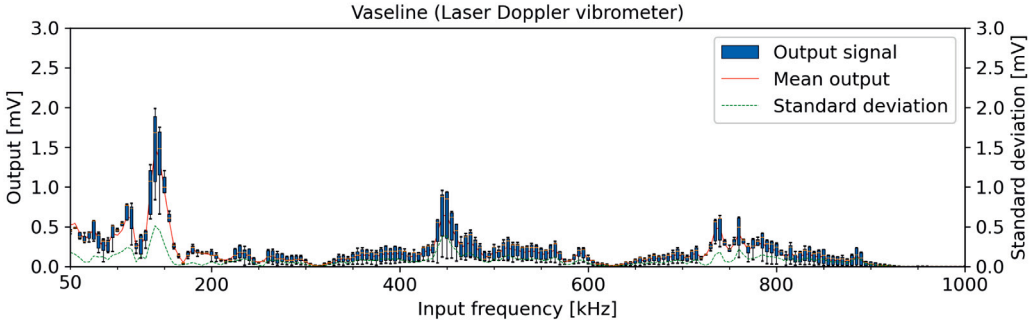

(d)

Fig. 6. Amplitude of output signals at input frequencies for the laser Doppler vibrometer measurements with different couplant materials: (a) reference measurement, (b) acrylic adhesive pads, (c) honey, and (d) vaseline.

low output signals in the reference measurement at these frequencies, which resulted in inflated values in the transfer function. Therefore, these high values should not be interpreted as real amplification, but rather as artifacts due to weak input signals at these frequencies.

The transfer functions of the VS30-V piezoelectric sensor coupled with different materials were determined using Eq. (8). As mentioned in Section 2.2.2, the transfer function analysis is intended for comparative purpose among the tested couplant materials within AE experiments

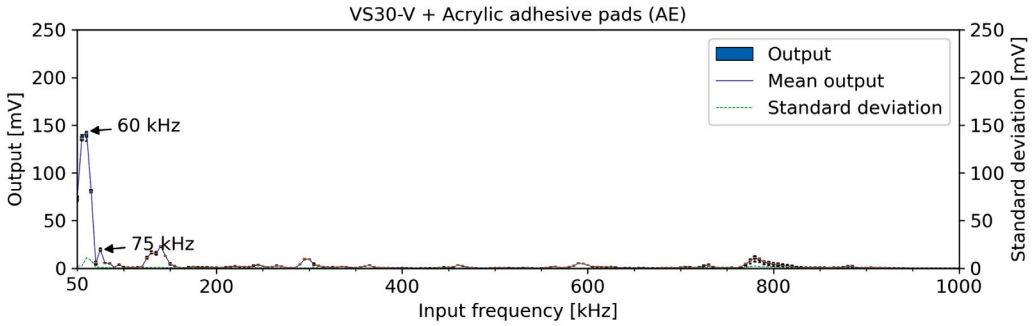

(a)

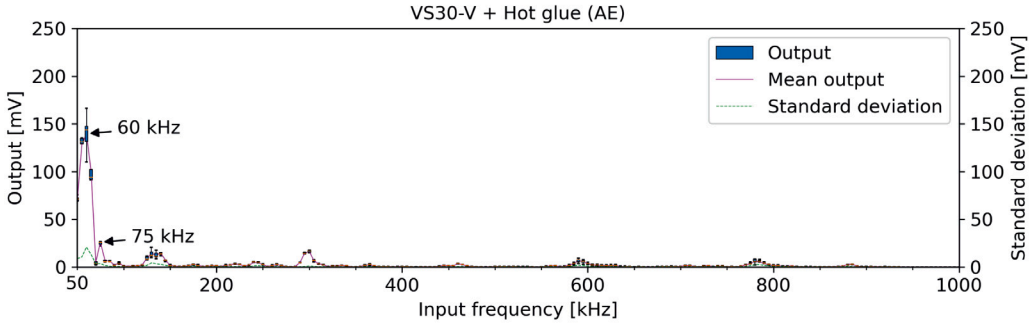

(b)

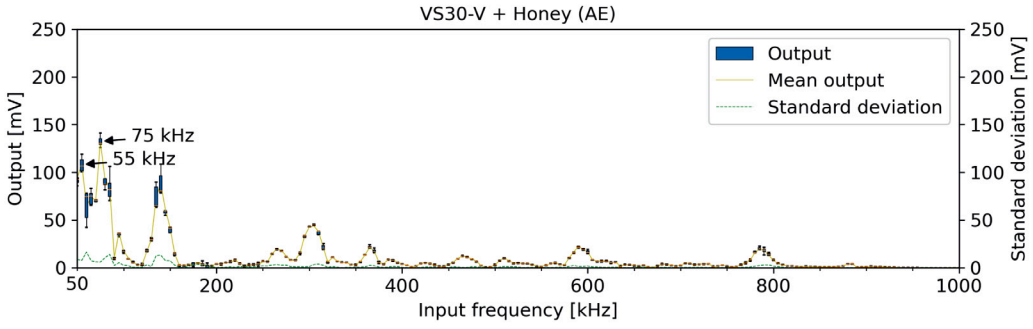

(c)

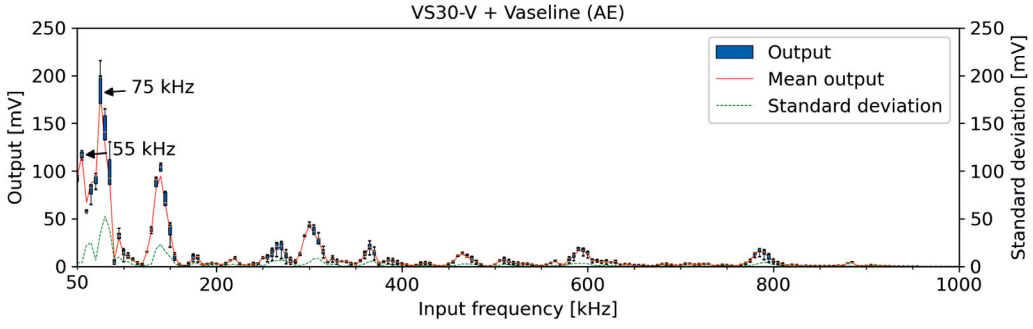

(d)

Fig. 7. Amplitude of output signals at input frequencies for the AE measurements with piezoelectric sensor VS30-V coupled with (a) acrylic adhesive pads, (b) hot glue, (c) honey, and (d) vaseline.

and should not be compared with the laser Doppler vibrometer measurements. Therefore, the computed transfer functions were normalized into the range [0, 1] and are presented in Fig. 10. It is worth mentioning that the transfer function computation was restricted to frequencies up to 850 kHz due to the digital filter in the AE measurements. Within the primary measuring range of the AE sensor (25 kHz–80 kHz), distinct trends were observed. In the low frequency range spanning from 50 kHz to 65 kHz, the transfer function of the AE sensor coupled with acrylic adhesive pads and hot glue displayed a slightly higher magnitude (1–2 times) compared to that of honey and vaseline. This observation implies

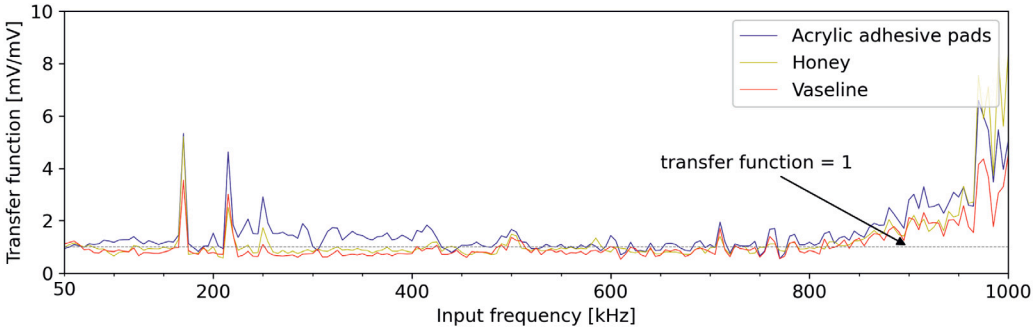

Fig. 8. Frequency dependent transfer functions of different couplant materials.

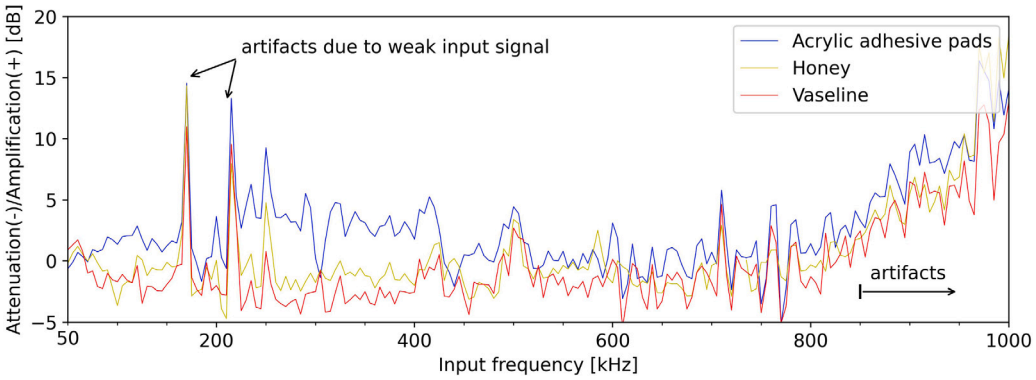

Fig. 9. Attenuation/Amplification of received signals with different couplant materials.

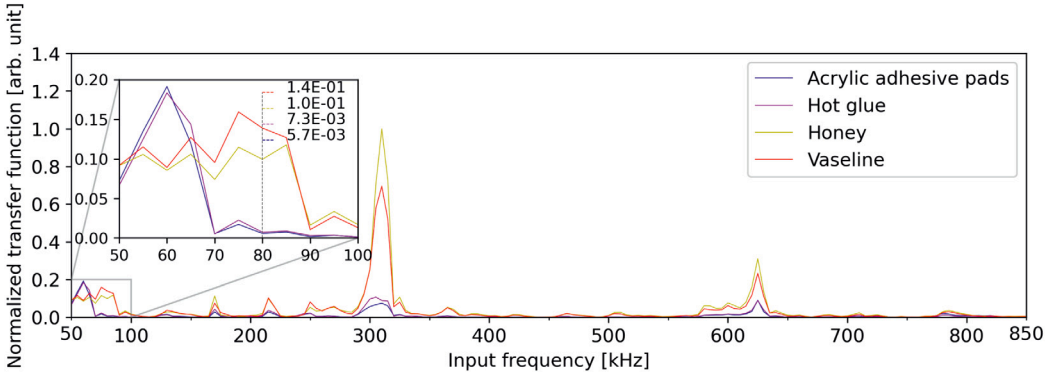

Fig. 10. Normalized frequency dependent transfer functions of the VS30-V sensor coupled with different materials.

that, within this frequency range, the impact of the couplant layer's thickness, which typically impedes signal transmission, is relatively insignificant. Conversely, the higher viscosity of acrylic adhesive pads and hot glue assumes greater influence on signal transmission, thereby contributing to the higher transfer function observed. From 65 kHz to 80 kHz, honey and vaseline exhibited significantly higher transfer functions with values up to 25 times greater, than those of acrylic adhesive pads and hot glue. This notable difference could be attributed to the thinner couplant layers employed. Beyond the main measuring range of the sensor, prominent peaks in transfer function were still obtained at specific frequencies, notably around 300 kHz and 630 kHz, which may be indicative of sensor resonance phenomena.

4. Conclusions

The quality and reliability of measurement data in non-destructive testing (NDT) depend largely on the coupling of sensors. This study analyzed the influence of various couplant materials, namely acrylic adhesive pads, hot glue, honey, and vaseline, on signal transmission in a piezoelectric sensor, as well as without sensor coupling. The frequency-dependent transfer functions of these materials were evaluated and compared. The main conclusions can be drawn as follows:

- The utilization of the investigated couplant materials, without sensor coupling, did not yield substantial amplification or damping effects on signal transmission.
- The assessment of the relative standard deviation (RSD) of the AE measurements indicates that acrylic adhesive pads exhibited the lowest RSD of 11.4% in the low-frequency range of 50 kHz to 100 kHz, followed by honey (13.2%), hot glue (21.9%) and vaseline (32.1%).
- In the frequency range of 50 kHz to 65 kHz, acrylic adhesive pads and hot glue exhibited higher transfer functions, up to two times greater than those of honey and vaseline. Considering the repeatability and ease of application of the couplant materials, acrylic adhesive pads are recommended for measurements in this frequency range.

- Between 65 kHz and 80 kHz, honey and vaseline displayed significantly higher transfer functions, up to 25 times greater compared to acrylic adhesive pads and hot glue. Considering the relatively greater variation observed in the vaseline experiments, honey emerges as a preferable choice within this frequency range.

The findings elucidated within this study are based on experiments conducted on a steel block under controlled laboratory conditions. In practical applications, the impact of factors such as steel surface roughness and the presence of coatings on the coupling interface should be subjected to further analysis. Moreover, additional research is required to apply these findings to diverse materials such as cementitious materials, which exhibit different attenuation and coupling properties than steel. In future research, another focus will be on investigating the impact of evolving environmental conditions over time on signal transmission, with particular attention given to the degradation of couplings. The objective is to comprehensively analyze how environmental factors, such as temperature, humidity, and mechanical stresses, affect the performance and reliability of couplings used in NDT applications. This will facilitate the evaluation of the durability of commonly used couplant materials in long-term structural health monitoring for civil engineering structures.

CRediT authorship contribution statement

Ronghua Xu: Conceptualization, Methodology, Software, Validation, Formal analysis, Investigation, Data curation, Writing – original draft, Writing – review & editing, Visualization. **Raúl Enrique Beltrán-Gutiérrez:** Conceptualization, Methodology, Investigation, Resources, Writing – review & editing. **Max Käding:** Conceptualization, Methodology, Resources, Writing – review & editing. **Alexander Lange:** Conceptualization, Methodology, Resources, Writing – review & editing. **Steffen Marx:** Conceptualization, Supervision. **Jörn Ostermann:** Conceptualization, Supervision.

Declaration of competing interest

The authors declare that they have no known competing financial interests or personal relationships that could have appeared to influence the work reported in this paper.

Data availability

Data is available in Mendeley Data Repository and has been cited in the manuscript.

Acknowledgment

This work was supported by German Federal Ministry for Economic Affairs and Climate Action (BMWK) [grant numbers: 03EE2025A].

References

[1] Elkarmoty M, Rupfle J, Helal K, Sholqamy M, Fath-Elbab M, Kollofrath J, et al. Localization and shape determination of a hidden corridor in the great pyramid of giza using non-destructive testing. NDT E Int 2023;139. http://dx.doi.org/10.1016/j.ndteint.2023.102809.

[2] Fröjd P, Ulriksen P. Amplitude and phase measurements of continuous diffuse fields for structural health monitoring of concrete structures. NDT E Int 2016;77:35–41. http://dx.doi.org/10.1016/j.ndteint.2015.10.003.

[3] Käding M, Schacht G, Marx S. Acoustic emission analysis of a comprehensive database of wire breaks in prestressed concrete girders. Eng Struct 2022;270:1–14. http://dx.doi.org/10.1016/j.engstruct.2022.114846.

[4] Lange A, Hinrichs R, Ostermann J. Localized damage detection in wind turbine rotor blades using airborne acoustic emissions. In: Materials research proceedings, Vol. 27. 2023, p. 228–35. http://dx.doi.org/10.21741/9781644902455-29.

[5] Aabid A, Parveez B, Raheman MA, Ibrahim YE, Anjum A, Hrairi M, et al. A review of piezoelectric material-based structural control and health monitoring techniques for engineering structures: Challenges and opportunities. Actuators 2021;10:1–26. http://dx.doi.org/10.3390/act10050101.

[6] Tuloup C, Harizi W, Aboura Z, Meyer Y, Khellil K, Lachat R. On the use of in-situ piezoelectric sensors for the manufacturing and structural health monitoring of polymer-matrix composites: A literature review. Compos Struct 2019;215:127–49. http://dx.doi.org/10.1016/j.compstruct.2019.02.046.

[7] Regtien P, Dertien E. Sensors for mechatronics. Elsevier; 2018, p. 267–303. http://dx.doi.org/10.1016/B978-0-12-813810-6.00009-4.

[8] Brunner AJ. Structural health and condition monitoring with acoustic emission and guided ultrasonic waves: What about long-term durability of sensors, sensor coupling and measurement chain? Appl Sci 2021;11:1–20. http://dx.doi.org/10.3390/app112411648.

[9] Ziegler B, Dudzik K. An overview of different possibilities to master the challenge of coupling an ae-sensor to an object of interest partly using examples of previous investigations. J KONES Powertrain Transp 2019;26:207–14. http://dx.doi.org/10.2478/kones-2019-0025.

[10] Richtlinie SE 02. Verifizierung von Schallemissionssensoren und ihrer Ankopplung im Labor. Technical Report, Berlin, Germany: DGZfP Fachausschuss Schallemissionsprüfverfahren (FA SEP); 2014.

[11] Dugmore K, Jonson D, Walker M. A comparison of signal consistency of common ultrasonic couplants used in inspection of composite structures. Compos Struct 2002;58:601–3. http://dx.doi.org/10.1016/S0263-8223(02)00131-9.

[12] Sun L, Kulkarni SS, Achenbach JD, Krishnaswamy S. Technique to minimize couplant-effect in acoustic nonlinearity measurements. J Acoust Soc Am 2006;120:2500–5. http://dx.doi.org/10.1121/1.2354023.

[13] ASTM E650/E650M-17. Standard guide for mounting piezoelectric acoustic emission sensors. Technical Report, West Conshohocken, Pennsylvania: ASTM International; 2017, http://dx.doi.org/10.1520/E0650_E0650M-17.

[14] Grosse CU. Evolution of NDT methods for structures and materials: Some success and failures. In: Nondestructive testing of materials and structures. 2013, p. 3–18. http://dx.doi.org/10.1007/978-94-007-0723-8_1.

[15] Colombo S, Giannopoulos A, Forde MC, Hasson R, Mulholland J. Frequency response of different couplant materials for mounting transducers. NDT E Int 2005;38:187–93. http://dx.doi.org/10.1016/j.ndteint.2004.03.008.

[16] Theobald P, Zeqiri B, Avison J. Couplants and their influence on ae sensor sensitivity. J Acoust Emiss 2008;26:91–7, URL https://www.ndt.net/?id=10884.

[17] Xu R, Käding M, Lange A, Ostermann J, Marx S. Detection of impulsive signals on tendons for hybrid wind turbines using acoustic emission measurements. In: International symposium on non-destructive testing in civil engineering (NDT-CE 2022), 16-18 August 2022, Zurich, Switzerland, Vol. 27. 2022, p. 1–10. http://dx.doi.org/10.58286/27292.

[18] Grosse CU, Schumacher T. Anwendungen der schallemissionsanalyse an betonbauwerken. Bautechnik 2013;90:721–31. http://dx.doi.org/10.1002/bate.201300074.

[19] Schumacher T, Linzer L, Grosse CU. Signal-based AE analysis. In: Acoustic emission testing. 2022, p. 73–116. http://dx.doi.org/10.1007/978-3-030-67936-1.

[20] Chung JY, Blaser DA. Transfer function method of measuring in-duct acoustic properties. I. Theory. J Acoust Soc Am 1980;68:907–13. http://dx.doi.org/10.1121/1.384778.

[21] Ono K, Cho H, Matsuo T. Transfer functions of acoustic emission sensors. J Acoust Emiss 2008;26:72–90, URL https://www.ndt.net/?id=10883.

[22] Ghaffari HO, Mok U, Pec M. On calibration of piezoelectric sensors with laser doppler vibrometer. J Acoust Soc Am 2021;150:2503–13. http://dx.doi.org/10.1121/10.0006445.

[23] Theobald P, Pocklington R. Velocity sensitivity calibration of AE sensors using the through wave method and laser interferometry. In: 29th European conference on acoustic emission testing, Vienna, Austria, September 8-10, 2010. 2010, URL https://www.ndt.net/?id=9741.

[24] Xu R. Effect of couplant materials on signal transmission. 2023, http://dx.doi.org/10.17632/k8xyz8jr7j.1, Mendeley Data, v1.